Pergamon

0277-5387(95)00162-X

Polyhedron Vol. 14, No. 20–21, pp. 2945–2951, 1995

0277-5387/95 $9.50+0.00

SYNTHESIS AND STRUCTURE OF INVERSE CYCLOOCTATETRAENYL SANDWICH COMPLEXES OF EUROPIUM(II): $[(C_5Me_5)(THF)_2Eu]_2(\mu\text{-}C_8H_8)$ AND $[(THF)_3K(\mu\text{-}C_8H_8)]_2Eu$

WILLIAM J. EVANS,* JULIE L. SHREEVE and JOSEPH W. ZILLER

Department of Chemistry, University of California at Irvine, Irvine, CA 92717, U.S.A.

(*Received* 9 *October* 1994; *accepted* 28 *March* 1995)

Abstract—The reaction of $K_2C_8H_8$ with $EuCl_3$, followed by reaction with KC_5Me_5 forms the Eu^{II} inverse sandwich complex $[(C_5Me_5)(THF)_2Eu]_2[\mu\text{-}(\eta^8:\eta^8\text{-}C_8H_8)]$ (**1**). A second type of Eu^{II} cyclooctatetraenyl species $\{(THF)_3K[\mu\text{-}(\eta^8:\eta^8\text{-}C_8H_8)]\}_2Eu$ (**2**), is generated when $K_2C_8H_8$ reacts with $Eu_3(OCMe_3)_7Cl_2(THF)_2$. Both **1** and **2** are symmetrically bridged complexes of the cyclooctatetraenyl dianion which contain formally 10-coordinate europium(II) metal centres.

Although the cyclooctatetraenyl ligand, $(C_8H_8)^{2-}$ (COT), was the crucial ligand which stimulated a renewal of interest in the organometallic chemistry of the *f* elements in 1968,[1,2] its subsequent use in *f* element chemistry has been less extensive than that of cyclopentadienyl ligands.[3–10] For example, although the synthesis of divalent lanthanide COT compounds was reported as early as 1969,[11] and an extensive organometallic chemistry is being developed for divalent lanthanides,[4] there are only three structurally characterized Ln^{II} COT complexes in the literature and these involve only ytterbium: $[K(DME)]_2[Yb\{\mu\text{-}(\eta^8:\eta^8\text{-}C_8H_8)\}_2]$,[12] $[K(diglyme)]_2[Yb\{\mu\text{-}(\eta^8:\eta^8\text{-}C_8H_7CMe_3)\}_2]$[13] and $(C_8H_8)Yb(py)_3$.[14]

Characterization of Ln^{II} COT complexes is difficult because neutral complexes of this dianionic ligand with divalent metals necessarily have only one ligand per metal centre. This generates a sterically unsaturated metal centre[4] which, in the absence of other donors, may polymerize to an insoluble material. Since Eu^{II} and Sm^{II} are larger than Yb^{II},[15] this problem is more difficult for these divalent ions. In this report, we describe the first two structurally characterized Eu^{II} COT complexes.

* Author to whom correspondence should be addressed.

EXPERIMENTAL

The compounds described below are extremely air- and moisture-sensitive and were handled under nitrogen with rigorous exclusion of air and water using standard Schlenk, vacuum line and glove box techniques. Complexes **1** and **2** decompose violently in air, as has been reported for other lanthanide cyclooctatetraene complexes.[14,16] All solvents were freshly distilled and dried as previously described.[17] Hydrated europium trichloride (Rhône-Poulenc) was dried[18] and $Eu_3(OCMe_3)_7Cl_2(THF)_2$ was prepared[19] according to the literature. 1,3,5,7-Cyclooctatetraene (Aldrich) was dried over activated 4 Å molecular sieves and was vacuum distilled before use. $K_2C_8H_8$ was prepared from potassium and 1,3,5,7-cyclooctatetraene according to literature methods.[16] ^1H NMR spectra were recorded on General Electric QE300 and GN500 instruments. IR spectra were recorded on a Perkin–Elmer 1600 series FT-IR. Elemental analysis was performed at Analytische Laboratorien GmbH, Fritz-Pregl-Strasse 24 D-5270 Gummersbach, Germany.

$[(C_5Me_5)(THF)_2Eu]_2(\mu\text{-}C_8H_8)$ (1)

In a glovebox, $K_2C_8H_8$ (350 mg, 1.9 mmol) was added to a suspension of $EuCl_3$ (496 mg, 1.9 mmol) in THF (*ca* 12 cm^3). The reaction mixture was stirred

for 18 h to give a red insoluble product. The red product was washed with THF and dried *in vacuo* (662 mg). Found: Eu, 42.0; C, 8.8; H, 0.8; Cl, 29.6; K, 17.9. Calc. for $Eu_3C_8H_8Cl_9K_5$: Eu, 42.4; C, 8.9; H, 0.7; Cl, 29.7; K, 18.2%.

The insoluble red product (300 mg) was slurried in THF and KC_5Me_5 (119 mg, 0.68 mmol) was added. After stirring for 12 h, the reaction mixture was centrifuged to remove an off-white insoluble product from the resulting bright orange solution. Removal of the solvent from the supernatant yielded a bright orange solid (317 mg, 0.33 mmol, 96% based on KC_5Me_5). Crystals suitable for X-ray analysis were obtained from a concentrated THF solution at −34°C. IR (neat): 2968 s, 2944 s, 2920 s, 2860 s, 1580 s br, 1433 m, 1371 m, 1353 m, 1311 m, 1258 w, 1084 s, 940 m, 797 s, 742 m, 665 s, 620 m cm^{-1}. ^1H NMR (THF-d_8): δ 50 to 35, and 15 to −10 ppm, broad lumps. Found: Eu, 31.2. Calc. for $Eu_2C_{44}H_{70}O_4$: Eu, 31.4%. Magnetic susceptibility (293 K, Evans' method[20]) $\chi_g = 5.9 \times 10^{-5}$ cgsu ($\mu_{eff} = 8.2\ \mu_B$).

$[(THF)_3K(\mu\text{-}C_8H_8)]_2Eu$ (2)

In a glovebox, a solution of $Eu_3(OCMe_3)_7Cl_2(THF)_2$, (300 mg, 0.25 mmol) in toluene (*ca* 5 cm^3) was added to a suspension of $K_2C_8H_8$ (139 mg, 0.76 mmol) in toluene (*ca* 5 cm^3). The reaction mixture became dark in colour and was stirred overnight. The mixture was centrifuged to give a green toluene solution and a dark insoluble fraction. The toluene insoluble fraction was extracted with THF (*ca* 10 cm^3) to give a dark red–brown solution. Removal of the THF by rotary evaporation left a dark red solid (86 mg). Cherry-red, X-ray quality crystals of **2** [179 mg, 27% based on $Eu_3(OCMe_3)_7Cl_2(THF)_2$] were grown from a concentrated THF solution at −34°C leaving behind a green solution. IR (neat): 3028 s, 3004 s, 2956 s, 2872 s, 1580 s br, 1454 w, 1406 m, 1382 m, 1352 m, 1250 w, 1203 s, 1052 s, 1029 s, 879 m, 799 s, 735 m, 669 s cm^{-1}. ^1H NMR (THF-d_8): δ-80 to -40, broad lump. Magnetic susceptibility (293 K, Evans' method[20]) $\chi_g = 2.8 \times 10^{-5}$ cgsu ($\mu_{eff} = 7.6\ \mu_B$).

General aspects of X-ray data collection, structure determination and refinement for 1 *and* 2

The determination of Laue symmetry, crystal class, unit cell parameters and the crystal's orientation matrix were carried out using standard techniques similar to those of Churchill.[21] Details are given in Table 1. All data were corrected for absorption and for Lorentz and polarization effects and were placed on an approximately absolute scale. Any reflection with $I(\text{net}) < 0$ was assigned the value $|F_o| = 0$. All crystallographic calculations were carried out using either our locally modified version of the UCLA Crystallographic Computing Package[22] or the SHELXTL PLUS program set.[23] The analytical scattering factors for neutral atoms were used throughout the analysis;[24] both the real ($\Delta f'$) and imaginary ($i\Delta f''$) components of anomalous dispersion were included. The quantity minimized during least-squares analysis was $\Sigma w(|F_o| - |F_c|)^2$ where w^{-1} is defined below. The structures were refined by full-matrix least-squares techniques. Hydrogen atoms were included using a riding model with $d(C—H) = 0.96$ Å and $U(\text{iso}) = 0.08$ Å.^{2}

$[(C_5Me_5)(THF)_2Eu]_2\{\mu\text{-}(\eta^8:\eta^8\text{-}C_8H_8)\}$ (**1**). A red–orange crystal of approximate dimensions $0.26 \times 0.28 \times 0.42$ mm was immersed in Paratone-

Table 1. Experimental data for the X-ray diffraction study of $[(C_5Me_5)(THF)_2Eu]_2[\mu\text{-}(C_8H_8)]$ (**1**) and $[(THF)_3K(\mu\text{-}C_8H_8)]_2Eu$ (**2**)

Compound	1	2
Formula	$C_{44}H_{70}O_4Eu_2$	$C_{40}H_{64}O_6K_2Eu$
FW	966.9	871.1
Temperature (K)	173	168
Crystal system	Monoclinic	Rhombohedral
Space group	*Pn*	$R\bar{3}$
a (Å)	11.0502(11)	14.9924(11)
b (Å)	13.9087(12)	
c (Å)	13.8156(12)	16.251(2)
β (°)	93.236(8)	
Volume (Å^3)	2120.0(3)	3163.4(6)
Z	2	3
D_{calcd} (Mg m^{-3})	1.515	1.372
Diffractometer	Siemens P3	Syntex $P2_1$
Data collected	$+h, +k, \pm l$	$\pm h, +k, +l$
Scan type	θ–2θ	ω
2θ Range (°)	4.0–50.0	4.0–45.0
μ(Mo-K_α), mm^{-1}	2.973	1.725
Reflections collected	4148	1498
Independent reflections	3938	917
Observed reflections	3938($|F_o| > 0$)	900($|F_o| > 3.0\sigma(|F_o|)$)
No. of variables	450	78
R_F (%)	3.0	3.4
R_{wF} (%)	4.1	4.5
Goodness of fit	1.11	1.11

Radiation: Mo-K_α ($\bar{\lambda} = 0.710730$ Å).
Monochomator: highly oriented graphite.
Scan range: 1.20° plus K_α separation.
Scan speed: 3.0° min^{-1} (in ω).

N under nitrogen[25] and transferred to a Siemens P3 diffractometer which is equipped with a modified LT-1 low-temperature system (173 K). An interruption in the nitrogen flow on the low-temperature device at the end of the data collection caused the crystal to decompose before absorption scans could be collected, and hence an absorption correction was done with the XABS program.[26] The reported refinement is that which has been corrected using the data generated by XABS. The diffraction symmetry was $2/m$ with systematic absences $h0l$ for $h+l = 2n+1$. The two possible monoclinic space groups are Pn and $P2/n$. It was later determined via successful solution and refinement of the model that the non-centrosymmetric space group Pn was correct. The quantity w^{-1} was defined as $\sigma^2(|F_o|)+0.0010(|F_o|)^2$.

The structure was solved by direct methods (SHELXTL PLUS) and refined by full-matrix least-squares techniques. Refinement of positional and thermal parameters led to convergence with $R_F = 3.0\%$, $R_{wF} = 4.1\%$ and GOF = 1.11 for 450 variables refined against all 3938 data with $|F_o| > 0$. A final difference-Fourier synthesis yielded $\rho(\max) = 1.11$ e Å^{-3}.

$\{(THF)_3K[\mu\text{-}(\eta^8:\eta^8\text{-}C_8H_8)]\}_2Eu$ (**2**). A red prism of approximate dimensions $0.20 \times 0.30 \times 0.30$ mm was mounted onto a glass fibre. The crystals were not stable in Paratone N at room temperature and desolvated very quickly when removed from the mother liquor at room temperature. The crystals were mounted at low temperature under nitrogen in the following way. A device was constructed so that a nitrogen-to-nitrogen (stream) transfer could be done. The mouth of a Buchner funnel was covered with porous tissue paper held in place with a rubber-band. The stem of the funnel was inserted into a two-hole rubber stopper which was inserted into a Dewar containing liquid nitrogen. Nitrogen gas introduced into the Dewar via the second hole was used to force a cold stream of nitrogen up and through the tissue paper. A pipette was used to transfer a mixture of the crystals and the mother liquor onto the cold tissue paper. Under a microscope, a crystal was selected and secured (with Paratone-N) to a glass fibre which was attached to an elongated brass mounting pin. The entire apparatus was carefully moved to the diffractometer where the mounted crystal was transferred from the nitrogen stream coming out of the Buchner funnel to the nitrogen stream of a Syntex $P2_1$ diffractometer (Siemens R3m/V System) which is equipped with a modified LT-1 low-temperature system (168 K). The diffraction symmetry indicated a rhombohedral crystal system with systematic absences for hkl where $-h-k+l = 3n+1$. The two possible space groups are the non-centrosymmetric $R3$ or the centrosymmetric $R\bar{3}$. The latter was chosen and determined to be correct by successful solution and refinement of the structure. The quantity w^{-1} was defined as $\sigma^2(|F_o|)+0.0010(|F_o|)^2$.

The structure was solved by direct methods (SHELXTL PLUS) and refined by full-matrix least-squares techniques. The molecule is located on a $\bar{3}$ centre of symmetry. The Eu atom is located at (0, 0, 0) with site-occupancy = 1/6. The K atom is at (0, 0, z; three-fold site symmetry) with site-occupancy = 1/3. The COT ring is rotationally disordered. There are three carbon components each of which has a site-occupancy of 8/9. Refinement of positional and thermal parameters led to convergence with $R_F = 3.4\%$, $R_{wF} = 4.5\%$ and GOF = 1.11 for 78 variables refined against those 900 data with $|F_o| > 3.0\sigma(|F_o|)$. A final difference-Fourier map was devoid of significant features, $\rho(\max) = 0.57$ e Å^{-3}.

RESULTS AND DISCUSSION

$[(C_5Me_5)(THF)_2Eu]_2(\mu\text{-}C_8H_8)$ (**1**)

Attempts to synthesize $(C_8H_8)EuCl(THF)_2$ from the reaction of $EuCl_3$ and $K_2C_8H_8$[16,27] yielded an insoluble red product whose elemental analysis was consistent with a mixture of the following components: $Eu(C_8H_8)$, 2 $EuCl_2$ and 5 KCl. Reduction of Eu^{III} to Eu^{II} has previously been observed with $C_5Me_5^-$[28] and hence reduction with $C_8H_8^{2-}$ is not improbable. The reaction of this insoluble product with KC_5Me_5 in THF yielded the bright orange, THF-soluble **1** in nearly quantitative yield based on the cyclopentadienyl reagent, eq. (1).

$$EuCl_3 \xrightarrow[2.\,KC_5Me_5]{1.\,K_2C_8H_8} [(C_5Me_5)(THF)_2Eu]_2[\mu\text{-}(\eta^8:\eta^8\text{-}C_8H_8)] \quad (1)$$

1

The structure of 1, Fig. 1, is that of an inverse sandwich in which the COT ring is located symmetrically between two Eu^{II} centres. Each europium has a formal coordination number of 10 due to one η^8-cyclooctatetraenyl moiety, one η^5-C_5Me_5 group and two THF ligands. The planar COT ring is nearly perpendicular to the Eu1—Eu2 vector: the Eu—(C_8H_8 centroid)—$C(C_8H_8)$ angles range from 88.0 to 93.6°. The C_5Me_5 rings are oriented in a transoid fashion with a [C_5Me_5] ring centroid)—Eu(1)—Eu(2)—(C_5Me_5 ring centroid) torsion angle of 78.3°. The (COT-ring centroid)—

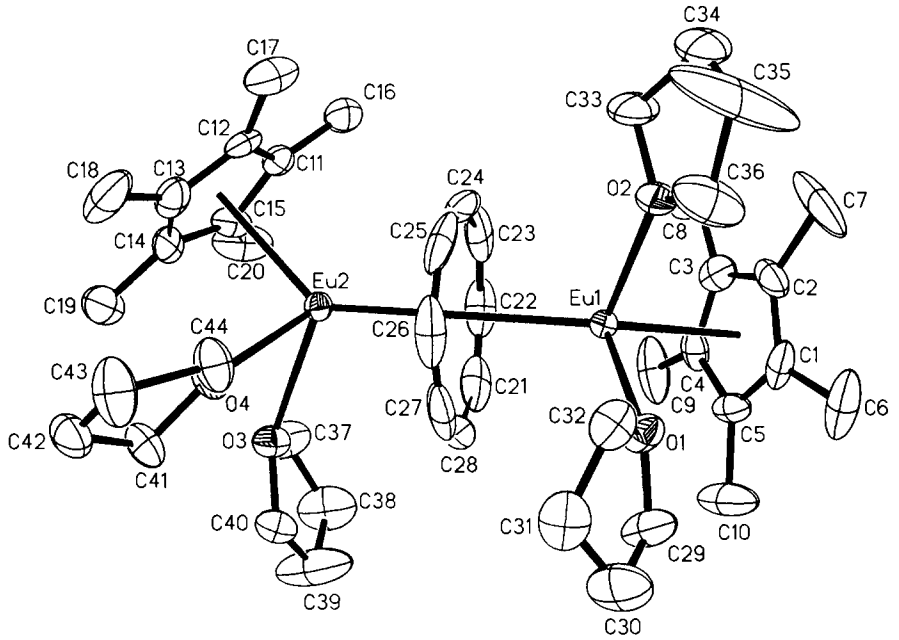

Fig. 1. Thermal ellipsoid plot of $[(C_5Me_5)(THF)_2Eu]_2[\mu\text{-}(\eta^8:\eta^8\text{-}C_8H_8)]$ (**1**) with probability ellipsoids drawn at the 50% level.

Eu—(C_5Me_5 ring centroid) angles are 139.1 and 137.9°.

Although a variety of lanthanide COT complexes have been reported and some inverse COT complexes are known, complex **1** displays uncommon structural features beyond the fact that it is the first structurally characterized Eu^{II} COT complex. Only two other examples of symmetrical inverse sandwich complexes of planar COT have been reported: $\{[(Me_3Si)_2N]_2Sm[\mu\text{-}(\eta^8:\eta^8\text{-}C_8H_8)]Sm[N(SiMe_3)_2]_2\}$,[29] and $\{[\mu\text{-}(\eta^8:\eta^8\text{-}C_8H_8)]K(THF)(\mu^2\text{-}THF)_2K\}_n$.[30] In addition, **1** is the first example of an inverse COT complex with cyclopentadienyl ligands and a rare example of a bent COT—C_5Me_5 complex. Although lanthanide COT complexes with small cyclopentadienyl ligands have bent structures, when larger cyclopentadienyl rings are present the angles tend toward linear. For example, 138.2 and 149.0° (COT ring centroid)—Ln—(C_5R_5 ring centroid) angles are found in $(C_8H_8)Pr(C_5H_5)$[31] and $(C_8H_8)Y(MeC_5H_4)(THF)$[32] whereas the analogous angles are 173.0° in $(C_8H_8)Lu(C_5Me_5)$[33] and 176.3 and 175.4° in $(C_8H_8)Lu(C_5Me_4H)$.[34] The only exception is the 135.66° angle in $(C_8H_8)La(C_5Me_4H)(THF)_2$.[34] These data and the structure of **1**, which show that larger metals and smaller cyclopentadienyl rings tend to form bent structures, suggest that the linear arrangement of rings appears to result when steric crowding occurs. A referee has pointed out that **1** can also be described as an analogue of a bent metallocene with two ligands $[(C_5R_5)_2ML_2]$ in that the two ring centroids and the two THF oxygen atoms define a distorted tetrahedron around each Eu.

Since, there are few divalent lanthanide cyclooctatetraenyl structures with which to compare structure parameters, data on the other ligands in **1** will be discussed first (Table 2). The 2.86(2) Å Eu(1)—C(C_5Me_5) and 2.878(7) Å Eu(2)—C(C_5Me_5) average distances in 10-coordinate **1** are numerically larger than the 2.79(1) Å average Eu—C(C_5Me_5) distance in six-coordinate $(C_5Me_5)_2Eu$,[35] although the range of the error limits overlaps. Considering that the Shannon radius[15] for 10-coordinate Eu^{II} is 0.18 Å larger than that for six-coordinate Eu^{II}, the Eu—C(C_5Me_5) distances in **1** are shorter than expected. Similarly, the 2.626(6)–2.688(7) Å range of Eu—O(THF) distances in **1** spans the 2.64(2) Å average Sm—O(THF) distance in eight-coordinate $(C_5Me_5)_2Sm(THF)_2$,[36] when it would be expected to be 0.08 Å larger based on Shannon radii. Hence, both metal–ligand distances involving ligands other than COT are smaller than expected.

The individual average Eu—C(C_8H_8) distances for Eu(1), 2.92 (3) Å, and Eu(2), 2.91 (6) Å, are statistically identical. These Eu—C(C_8H_8) averages in **1** are reasonable compared with the 2.74 (3) Å average Yb—C(C_8H_8) distance in 10-coordinate $[K(DME)]_2[Yb\{\mu\text{-}(\eta^8:\eta^8\text{-}C_8H_8)\}_2]$,[12] the 2.77 (4) Å average in $[K(diglyme)]_2[Yb\{\mu\text{-}(\eta^8:\eta^8\text{-}C_8H_7CMe_3)\}_2]$[13] and the 2.64 (3) Å average in seven-

Table 2. Selected interatomic distances (Å) and angles (°) for $[(C_5Me_5)(THF)_2Eu]_2(\mu\text{-}C_8H_8)$ (**1**)

Eu(1)—O(1)	2.650(6)	Eu(2)—O(3)	2.688(7)
Eu(1)—O(2)	2.680(7)	Eu(2)—O(4)	2.626(6)
Eu(1)—C(1)	2.881(10)	Eu(2)—C(11)	2.872(8)
Eu(1)—C(2)	2.855(10)	Eu(2)—C(12)	2.883(8)
Eu(1)—C(3)	2.826(9)	Eu(2)—C(13)	2.881(10)
Eu(1)—C(4)	2.839(9)	Eu(2)—C(14)	2.868(9)
Eu(1)—C(5)	2.878(9)	Eu(2)—C(15)	2.884(9)
Eu(1)—C(21)	2.898(14)	Eu(2)—C(21)	2.978(12)
Eu(1)—C(22)	2.948(14)	Eu(2)—C(22)	2.909(11)
Eu(1)—C(23)	2.881(11)	Eu(2)—C(23)	2.890(14)
Eu(1)—C(24)	2.898(13)	Eu(2)—C(24)	2.856(14)
Eu(1)—C(25)	2.962(13)	Eu(2)—C(25)	2.850(14)
Eu(1)—C(26)	2.974(10)	Eu(2)—C(26)	2.878(16)
Eu(1)—C(27)	2.918(14)	Eu(2)—C(27)	2.982(12)
Eu(1)—C(28)	2.924(12)	Eu(2)—C(28)	3.024(12)
O(1)—Eu(1)—O(2)	82.2(2)	O(3)—Eu(2)—O(4)	77.4(2)
O(1)—Eu(1)—C(1)	77.3(2)	O(3)—Eu(2)—C(11)	115.5(2)
O(2)—Eu(1)—C(1)	89.5(3)	O(4)—Eu(2)—C(11)	122.0(2)
O(1)—Eu(1)—C(2)	99.0(3)	O(3)—Eu(2)—C(12)	129.6(2)
O(2)—Eu(1)—C(2)	74.3(3)	O(4)—Eu(2)—C(12)	97.8(2)
C(1)—Eu(1)—C(2)	28.6(3)	C(11)—Eu(2)—C(12)	28.7(2)
O(1)—Eu(1)—C(3)	124.3(2)	O(3)—Eu(2)—C(13)	107.3(3)
(COT centroid)—Eu(1)—(C_5Me_5 centroid)		139.1	
(COT centroid)—Eu(2)—(C_5Me_5 centroid)		137.9	
(COT centroid)—Eu(1)—O(1)		110.3	
(COT centroid)—Eu(1)—O(2)		110.5	
(COT centroid)—Eu(2)—O(3)		108.7	
(COT centroid)—Eu(2)—O(4)		112.6	
(C_5Me_5 centroid)—Eu(1)—O(1)		100.9	
(C_5Me_5 centroid)—Eu(1)—O(2)		99.3	
(C_5Me_5 centroid)—Eu(2)—O(3)		105.2	
(C_5Me_5 centroid)—Eu(2)—O(4)		98.4	

coordinate $(C_8H_8)Yb(py)_3$,[14] when the differences in metallic radii and coordination number are taken into consideration.[15] The 2.850 (14)–3.024 (12) Å range of Eu—C(C_8H_8) distances in **1** is larger and broader than the 2.791 (14)–2.809 (10) Å range of Eu—C(C_8H_8) distances in **2** which is also 10-coordinate (see below).

$[K(THF)_3(\mu\text{-}C_8H_8)]_2Eu$ (**2**)

The reaction of $K_2C_8H_8$ with $Eu_3(OCMe_3)_7Cl_2(THF)_2$ in toluene yields a mixture of products from which **2** can be readily separated by crystallization from THF. As shown in Fig. 2, the europium atom in **2** is symmetrically sandwiched between the two planar COT rings, which in turn are sandwiched between the Eu and a $K(THF)_3$ unit. The highly symmetrical complex crystallized in the $R\bar{3}$ space group which is unusual for a COT-containing molecule which would be expected to have even rather than odd rotational symmetry. Compound **2** has a molecular S_3 axis which passes through Eu and K and the COT rings are rotationally disordered. Three unique carbon positions, each with 8/9 occupancy, generate the COT ring. By symmetry, the COT rings are perpendicular to the K(1)—Eu(1)—K(1a) vector.

The three independent Eu—C(C_8H_8) distances (Table 3), 2.791(14), 2.780(27) and 2.809(10) Å, are very similar. The 2.79(3) Å average distance is about 0.05 Å shorter than would be expected in comparison with the 2.74(3) Å average Yb—C(C_8H_8) distance in $[K(DME)]_2[Yb(C_8H_8)_2]$,[12] and the 2.77(4) Å average in $[K(diglyme)]_2[Yb\{\mu\text{-}(\eta^8:\eta^8\text{-}C_8H_7CMe_3)\}_2]$,[13] when the differences in metallic radii are considered.[15] However, this difference is not statistically significant considering the error limits on the bond distances.

The average K—C(C_8H_8) distance is 3.01 (2) Å,

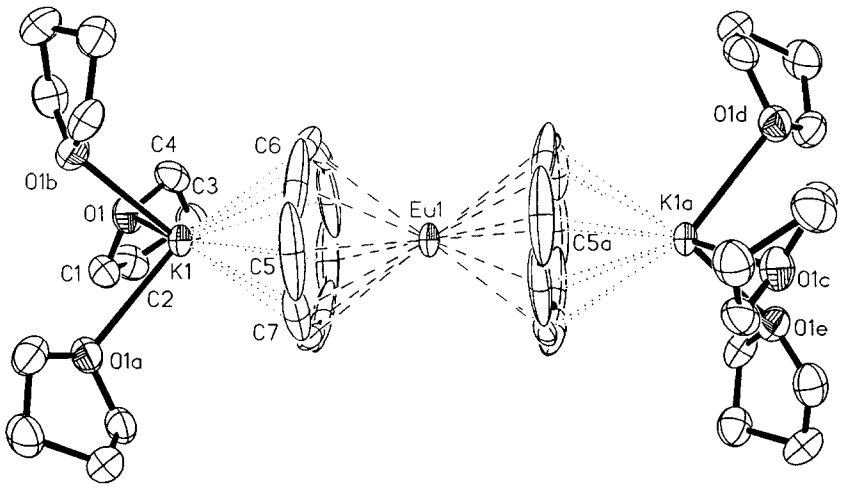

Fig. 2. Thermal ellipsoid plot of $\{(THF)_3K[\mu\text{-}(\eta^8:\eta^8\text{-}C_8H_8)]\}_2Eu$ (**2**) with probability ellipsoids drawn at the 50% level.

Table 3. Selected interatomic distances (Å) and angles (°) for $[(THF)_3K(\mu\text{-}C_8H_8)]_2Eu$ (**2**)

Eu(1)···K(1)	4.574(2)	K(1)—O(1)	2.701(4)
Eu(1)—C(5)	2.791(14)	K(1)—C(5)	3.014(13)
Eu(1)—C(6)	2.780(27)	K(1)—C(6)	3.018(25)
Eu(1)—C(7)	2.809(10)	K(1)—C(7)	2.985(10)
Eu(1)—centroid	2.153	K(1)—centroid	2.422
K(1)—Eu(1)—K(1A)	180.0(1)	Eu(1)—K(1)—O(1)	125.8(1)
O(1)—K(1)—centroid	125.8	O(1)—K(1)—O(1A)	89.3(1)
K(1)—O(1)—C(1)	116.1(2)	K(1)—O(1)—C(4)	115.8 (3)
C(6)—C(5)—C(7)	139.3(26)	C(5)—C(7)—C(6D)	140.3(20)
C(5)—C(6)—C(7B)	140.2(39)		

Centroid = centroid of the $C_8H_8^{2-}$ ring system.

which compares well with the analogous distances of 3.02(2) Å in $[K(DME)]_2[Yb(C_8H_8)_2]$,[12] 3.08 (5) Å in $[K(diglyme)]_2[Yb\{\mu\text{-}(\eta^8:\ \eta^8\text{-}C_8H_7CMe_3)\}_2]$[13] and 3.003(8) Å in $[K((CH_3OCH_2CH_2)_2O)]_2[C_8H_4Me_4]$.[37] This distance is statistically similar to the ranges of K—C(C_8H_8) values of 3.024 (16)–3.153 (10) and 3.130 (12)–3.284 (13) Å observed in $[\mu\text{-}(\eta^8\text{-}C_8H_8)]Er[\mu\text{-}(\eta^8:\eta^8\text{-}C_8H_8)]K[\mu\text{-}(\eta^8:\eta^8\text{-}C_8H_8)]Er[\mu\text{-}(\eta^8:\eta^8\text{-}C_8H_8)]K(THF)_4$ (**3**).[38] The 2.701(4) Å K—O(THF) distance is similar to the 2.692 (2) Å average K—O(THF) distance in **3**[38] and the 2.665 (6) Å distance in $\{[\mu\text{-}(\eta^8:\eta^8\text{-}C_8H_8)]K(THF)(\mu^2\text{-}THF)_2K\}_n$.[30]

CONCLUSION

Soluble, structurally characterizable, non-polymeric Eu^{II} COT complexes can be obtained by generating the Eu^{II}(COT) unit in the presence of ancillary moieties which will either add to the coordination number of Eu^{II} when the COT/Eu ratio is ≤ 1 or coordinate to the side of the COT ligands opposite Eu^{II} when the COT/Eu ratio is 2. Such complexes are conveniently obtained from trivalent precursors, a reaction which is not unexpected considering the ease of Eu^{III} to Eu^{II} reduction and the reducing capacity of the cyclooctatetraenyl dianion. The structural features of **1** and **2** suggest that a wide variety of coordination modes involving COT ligands are possible with the divalent lanthanides.

Acknowledgements—We thank the National Science Foundation for support of this research.

REFERENCES

1. A. Streitwieser, Jr and U. Müller-Westerhoff, *J. Am. Chem. Soc.* 1968 **90**, 7364.
2. F. Mares, K. Hodgson and A. Streitwieser, Jr, *J. Organomet. Chem.* 1970, **24**, C68.

3. W. J. Evans, *Adv. Organomet. Chem.* 1985, **24**, 131, and references therein.
4. W. J. Evans, *Polyhedron* 1987, **6**, 803, and references therein.
5. P. L. Watson and G. W. Parshall, *Acc. Chem. Res.* 1985, **18**, 51, and references therein.
6. H. Schumann and W. Genthe, in *Handbook on the Physics and Chemistry of Rare Earths* (Edited by K. A. Gschneidner, Jr and L. Eyring), Vol. 7, Ch. 53. Elsevier: Amsterdam (1985), and references therein.
7. T. J. Marks and R. D. Ernst, in *Comprehensive Organometallic Chemistry* (Edited by G. Wilkinson and F. G. A. Stone), Vol. 3, Ch. 21. Pergamon Press, Oxford.
8. J. H. Forsberg and T. Moeller, in *Gmelin Handbook of Inorganic Chemistry*, 8th edn (Edited by T. Moeller, U. Kruerke and E. Schleitzer-Rust), Part D6, 137. Springer-Verlag, Berlin (1983).
9. H. B. Kagan and J. L. Namy, in *Handbook on the Physics and Chemistry of Rare Earths* (Edited by K. A. Gschneidner, Jr and L. Eyring) Vol. 7, Ch. 50. Elsevier, Amsterdam (1985), and references therein.
10. C. J. Schaverien, *Adv. Organomet. Chem.* 1994, **36**, 283, and references therein.
11. R. G. Hayes and J. L. Thomas, *J. Am. Chem. Soc.* 1969, **91**, 6876.
12. S. A. Kinsley, A. Streitwieser, Jr and A. Zalkin, *Organometallics* 1985, **4**, 52.
13. S. A. Kinsley, A. Streitwieser, Jr and A. Zalkin, *Acta Cryst.* 1986, **C42**, 1092.
14. A. L. Wayda, I. Mukerji, J. L. Dye and R. D. Rogers, *Organometallics* 1987, **6**, 1328.
15. R. D. Shannon, *Acta Cryst.* 1976, **A32**, 751–767.
16. A. L. Wayda, *Inorg. Synth.*, Vol. 27 (Edited by A. P. Ginsberg), pp. 150–154.
17. W. J. Evans, L. R. Chamberlain, T. A. Ulibarri and J. W. Ziller, *J. Am. Chem. Soc.* 1988, **110**, 6423.
18. M. D. Taylor and C. P. Carter, *J. Inorg. Nucl. Chem.* 1962, **24**, 387.
19. W. J. Evans, J. L. Shreeve and J. W. Ziller, *Organometallics* 1994, **13**, 731.
20. D. F. Evans, *J. Chem. Soc.* 1959, 2003; J. K. Beccon-sall, *Mol. Phys.* 1968, **15**, 129.
21. M. R. Churchill, R. A. Lashewycz and F. J. Rotella, *Inorg. Chem.* 1977, **16**, 265.
22. UCLA Crystallographic Computing Package, University of California, LA (1981); C. Strouse, personal communication.
23. Siemens Analytical X-ray Instruments, Inc., Madison, WI (1990).
24. *International Tables for X-ray Crystallography*; (a) pp. 99–101; (b) pp. 149–150. Kynoch Press: Birmingham, England (1974).
25. H. Hope, *Experimental Organometallic Chemistry: A Practicum in Synthesis and Characterization*, ACS Symposium Series No. 357 (Edited by A. L. Wayda and M. Y. Darensbourg) (1987).
26. XABS program courtesy of Professor Hakon Hope, University of California, DA (1980).
27. F. Mares, K. Hodgson and A. Streitwieser, Jr, *J. Organomet. Chem.* 1971, **28**, C24.
28. T. D. Tilley, R. A. Andersen, B. Spencer, H. Ruben, A. Zalkin and D. H. Templeton, *Inorg. Chem.* 1980, **19**, 2999.
29. H. Schumann, J. Winterfeld, L. Esser and G. Kociok-Köhn, *Angew. Chem., Int. Edn Engl.* 1993, **32**, 1208.
30. N. Hu, L. Gong, Z. Jin and W. Chen, *J. Organomet. Chem.* 1988, **352**, 61.
31. K. Wen, Z. Jin and W. Chen, *J. Chem. Soc., Chem. Commun.* 1991, 680.
32. H. Schumann, J. Sun and A. Dietrich, *Monatsh. Chem.* 1990, **121**, 747.
33. H. Schumann, R. D. Köhn, F.-W. Reier, A. Dietrich and J. Pickardt, *Organometallics* 1989, **8**, 1388.
34. H. Schumann, M. Glanz, J. Winterfield and H. Hemling, *J. Organomet. Chem.* 1993, **456**, 77.
35. W. J. Evans, L. A. Hughes and T. P. Hanusa, *Organometallics* 1986, **5**, 1285.
36. W. J. Evans and S. E. Foster, *J. Organomet. Chem.* 1992, **433**, 79.
37. S. Z. Goldberg, K. N. Raymond, C. A. Harmon and D. H. Templeton, *J. Am. Chem. Soc.* 1974, **96**, 1348.
38. J. Xia, Z. Jin and W. Chen, *J. Chem. Soc., Chem. Commun.* 1991, 1214.